Journal of
Materials Chemistry C

Accepted Manuscript

Volume 4 | Number 1 | 7 January 2016 | Pages 1–224

Journal of
Materials Chemistry C

Materials for optical, magnetic and electronic devices
www.rsc.org/MaterialsC

ISSN 2050-7526

PAPER
Nguyễn T. K. Thanh, Xiaodi Su et al.
Fine-tuning of gold nanorod dimensions and plasmonic properties using the Hofmeister effects

175 YEARS

ROYAL SOCIETY
OF CHEMISTRY

rsc.li/materials-c

Dynamic nature of excited states of donor-acceptor TADF materials for OLEDs: how theory can reveal structure-property relationships.

Yoann Olivier [*]   Mónica Moral [†]   Luca Muccioli [‡§]
Juan-Carlos Sancho-García [¶]

December 8, 2016

[*]Laboratory for Chemistry of Novel Materials, University of Mons, 7000 Mons, Belgium, E-mail: `yoann.olivier@umons.ac.be`

[†]Renewable Energy Research Institute University of Castilla-La Mancha, 02071 Albacete, Spain

[‡]Institut des Sciences Moléculaires, UMR 5255, University of Bordeaux, 33405 Talence, France

[§]Dipartimento di Chimica Industriale "Toso Montanari", University of Bologna, 40136 Bologna, Italy

[¶]Departamento de Química Física, University of Alicante, 03080 Alicante, Spain

1

Journal of Materials Chemistry C Accepted Manuscript

Abstract

Spin statistics greatly limits the efficiency of OLEDs, which might be largely improved upon conversion of triplet into singlet-excited (and thus light-emitting) states via a Thermally Activated Delayed Fluorescence (TADF) process. We theoretically investigate here the combination of some real-life Donor (D) and Acceptor (A) moieties with the connectivity D-A and D-A-D. We selected phenoxazine (PXZ) and phenylthiazine (PTZ) as electron-donating groups, and 2,5-diphenyl-1,3,4-oxadiazole (OXD), 3,4,5-triphenyl-4H-1,2,4-triazole (TAZ), and 2,5-diphenyl-1,3,4-thiadiazole (TDZ) as their electron-accepting partners. The systematic Tamm-Dancoff Approximation-Density Functional Theory calculations performed have allowed us to calculate accurately not only the energy levels of low-lying singlet and triplet-excited states, but also to characterize their Charge-Transfer (CT) or Locally Excited (LE) nature, since the energy difference and the coupling between the ^3CT, ^3LE, and ^1CT states becomes key to understand the molecular mechanism involved in this process. We have also studied the role played by the conformational landscape, arising from the thermally accessible range of D-A(-D) torsion angles, in the singlet-triplet energy gap as well as its influence on oscillator strengths. Overall, we rationalize the origin of the higher efficiencies found in real devices for D-A-D molecules, disclosing the underlying structure-property relationships and thus anticipating successful de-

sign strategies.

1 Introduction

The development of Organic Light-Emitting Diodes (OLEDs) has followed a constant and rapid improvement over the recent years, leading already to the first market applications. On the way to produce OLEDs for lighting, or multicolor displays, materials able to emit in the red, green and blue regions of the visible spectrum have to be synthesized and the corresponding device efficiently manufactured.[1–4] State-of-the-art OLEDs have a multi-layer architecture where the most important role is played by hole/electron injecting layers, to ease charge injection, and hole/electron blocking layers, to confine the charge carriers to the EMitting Layer (EML). When focusing on the EML, the main factor inhibiting the Internal Quantum Efficiency (IQE) is the unfavorable spin statistics when charges combine to form excitons.[5,6] Indeed, only 25 % of light emitting singlet excited-states (S_1) versus the 75 % of non-emissive triplet excited-states (T_1) are created, limiting the external quantum efficiency (EQE) of fluorescent emitters to 5 % when considering an out-coupling efficiency of 20 %. So far, one of the most employed strategy in order to maximize the IQE of these devices, relies on the use of compounds containing heavy metals such as Iridium or Platinum with a large spin-orbit coupling, making phosphorescence activity (emission from the in principle dark T_1 state) reliable enough, thus avoiding energy losses through non-radiative processes.[7]

As an alternative to the use of costly and/or possibly toxic phosphorescent metal complexes, new fully organic materials relying on the Thermally Activated Delayed Fluorescence (TADF) mechanism have been recently developed[8–11] to ease the conversion of the non-emissive triplet excitons to

emissive singlet states by a (Reverse) InterSystem Crossing ((R)ISC) mechanism. In TADF materials, the usual prompt fluorescence occurring on the sub-nanosecond timescale is followed by a long-lived component typically on the micro- to the millisecond scale, the so-called delayed fluorescence resulting from the interconversion of triplet excitons into singlets. Knowing that phosphorescent compounds are able to achieve an External Quantum Efficiency (EQE) close to 30 %,[12,13] competitive values around 30 % have been already obtained[5] for devices made of purely organic host matrices and TADF green emitters, while blue emitters are still lagging behind with EQE around 20 %[14] leaving thus room for further improvements.

The general strategy to maximize the conversion of triplets into singlets consists in minimizing the spatial overlap between the HOMO (Highest Occupied Molecular Orbital) and LUMO (Lowest Unoccupied Molecular Orbital) frontier orbitals in order to minimize the exchange energy and bring the singlet and triplet excited states close together. This is usually achieved in Donor-Acceptor (D-A) compounds where the HOMO (LUMO) is primarily localized on the donor (acceptor) moiety. As a consequence of this large spatial separation, the lowest singlet and triplet excitations usually feature a strong intramolecular charge-transfer (ICT) character, which is not always compatible with intense emission requirements (high oscillator strength and large transition dipole moment).[15] The choice of the donor and the acceptor appears to be very crucial since in some instances, a Locally Excited triplet state (^3LE) localized either on the donor or the acceptor becomes more stable than the charge transfer (CT) states, thus hindering the triplet to singlet interconversion and leading to inefficient TADF.[16] Up to now, the main picure that has arisen to explain the TADF mechanism involves the interconversion between ^3CT and ^1CT states.[2–6] However, more recently Monkman and co.

have hypothesized a key role of the presence of a ^3LE state in near resonance with the CT states, which might lead to an enhancement of the interconversion mechanism. This appears to be a consequence of a larger ^3LE-^1CT spin-orbit coupling in comparison to the ^3CT-^1CT one, because of the different spatial localization of the involved states.[17–19] As an alternative to these mechanisms driven by spin-orbit coupling, interconversion driven by hyperfine couplings has also been reported but appears to be a negligible pathway since its contribution requires an energy spacing between the ^3CT and ^1CT states below 1 cm^{-1}.[20] Even though the detailed mechanism of TADF is still under debate, the interconversion between triplet and singlet excitons clearly involves excited states carrying a significant CT character.

On the computational side, identifying and benchmarking a protocol capable of accurately estimating the difference in energy between the singlet and triplet states, as well as of classifying their nature (either LE or CT) for designing promising materials, remains a challenging task because of the lack of a well-established methodology able to simultaneously describe (sin-glet and triplet) CT states. Since the presence of ICT states seems to be co-substantial with the nature itself of an efficient interconversion mecha-nism, the blind application of density functional theory (DFT) remains a challenge, and thus fine-tuned exchange-correlation functional are used, that is employing a different weight of exact-like exchange[21] or optimizing the range-separation parameter[22,23] for each compound, making this procedure not transferable to new candidates.[21] With a somewhat different goal, recent studies pursued the computational screening of any possible host/guest system from a set of defined fragments without any experimental information, through the use of machine-learning approaches able to identify the potential of candidate emitters when used in devices.[24,25] Even though this approach

might be highly useful for initial studies of unknown molecules, or for preliminary or blind screening, it still suffers from reported uncertainties of around ± 0.3 eV in the evaluation of the ΔE^{ST}, the energy gap between the singlet and triplet lowest excited states, and calls for more accurate estimates to disclose any molecular design rules.

So far, the most common strategy for designing new TADF emitters relies on the Donor-Acceptor (D-A) approach.[26] The amount of electronic interaction between these moieties needs to be well-balanced in order to obtain the singlet and triplet CT (as well as the ^3LE) states close in energy and HOMO (LUMO) orbital mainly localized on the donor (acceptor) unit. The D-A electronic interaction can be tuned by engineering (i) the energy offset between the frontiers orbitals, (ii) the molecular symmetry, (iii) the geometrical and sterical constraints (i.e. dihedral angle between the D and the A) and (iv) by using a connector between them. However the final outcome is always a compromise between the contrasting requirements of spacial separation of the orbitals (to minimize ΔE^{ST}) and a non-negligible overlap (to gain sufficient oscillator strength and make light emission possible).

Besides D-A materials where a single D is grafted to the A unit, recent literature demonstrates the rise of compounds where several donors are attached to the acceptor unit, achieving low ΔE^{ST} and presenting particularly high EQEs.[5,14,27–29] Adachi and co. have synthesized symmetric D-A-D compounds containing phenoxazine (PXZ) as electron donor, and 2,5-diphenyl-1,3,4-oxadiazole (OXD) as electron acceptor, 2PXZ-OXD, or 3,4,5-triphenyl-4H-1,2,4-triazole (TAZ) as acceptor, 2PXZ-TAZ. Those D-A-D have shown PhotoLuminescence Quantum Yields (PLQYs) larger than their D-A parent compounds (i.e. PXZ-OXD and PXZ-TAZ) in toluene solution.[30] In addition, 2PXZ-TAZ and PXZ-TAZ are quite remarkable since they display sky

blue-emission, a feature of a particular interest considering the relatively few available blue TADF emitters.[14] With a similar molecular design approach, the same authors have also introduced 2,5-diphenyl-1,3,4-thiadiazole (TDZ) to replace OXD, leading to a reduced ΔE^{ST}, a shift to the orange of the emission maximum and an increased contribution of the delayed component of the fluorescence to the EQE, attributed to a reduced ΔE^{ST} in comparison to 2PXZ-OXD.[31]

Since we have recently benchmarked a methodology[32] able to provide deviations as low as 0.1 eV for the ΔE^{ST} energy gap with respect to experimental results, in this study we aim at applying it to the characterization the excited states properties of (2)PXZ-OXD and (2)PXZ-TAZ compounds. Owing to the relative simple structure of the D-A(-D) compounds we have systematically changed the nature of the electron-donating and accepting groups to study their impact on the magnitude of the ΔE^{ST}. We consider in addition to PXZ, phenothiazine (PTZ) as a second donor. Analogous to PXZ, PTZ is a convenient electron donor in various applications such as dye-sensitized solar cells,[33,34] polymer field-effect transistors[35] and light-emitting diodes.[36–38] Similarly, we have increased the strength of the acceptor group by investigating TAZ, OXD and TDZ, respectively. The combination of the different electron donors and acceptors result in six D-A and six D-A-D molecules (see Figure 1), whose excited and ground states are thouroughly characterized in the following. In addition, since it was previously[39] shown when considering PTZ as an electron donor and a triphenyl-triazine electron acceptor (TRZ) that PTZ-TRZ exists in two distinct conformations, namely the (quasi-)axial (almost coplanar D and A units) and the (quasi-)equatorial (large torsion angle between the D and A units) conformations, we consider and compare both conformers for all compounds.

8

2 Computational details

We optimize in all cases the ground-state (S_0) geometry of the compounds with the PBE0-D3(BJ) method,[40,41] including the -D3(BJ) correction for intra-molecular (if any) dispersion effects.[42–44] We then compute the vertical excitation energies for absorption to the S_1 $(E_V(S_1))$ and T_1 $(E_V(T_1))$ excited-states which gives correspondingly the vertical singlet-triplet gap as $\Delta E_V^{ST} = E_V(S_1) - E_V(T_1)$. We also calculate the adiabatic $\Delta E_A^{ST} = E(S_1) - E(T_1) = \Delta E_V^{ST} - \lambda_{S_1} + \lambda_{T_1}$ where λ_{S_1} and λ_{T_1} are the relaxation energies calculated in the S_1 and T_1 state and which are calculated as $\lambda_{S_1} = E_V(S_1) - E(S_1)$ and $\lambda_{T_1} = E_V(T_1) - E(T_1)$ where $E(S_1)$ and $E(T_1)$ represent the energy of the optimized S_1 and T_1 states, respectively. All excited states energies (relaxed and unrelaxed) are calculated within the Tamm-Dancoff approximation (TDA)[45] to the linear-response time-dependent (TD-)DFT approach, which significantly and systematically improves the accuracy of triplet energies[46–48] and ΔE^{ST} values. We consequently include solvent effects by the non-equilibrium Polarizable Continuum Model (PCM) using the integral equation formalism variant (IEF-PCM) for hybrid (i.e. PBE0) methods both for the geometry optimization and excited state calculations.[49,50] All calculations have been performed with the GAUSSIAN09 D.01 package.[51] In order to choose the basis set we have compared in Tables S1 and S2 the 6-31G(d,p) and def2-TZVP[52] ones and verified that they lead to similar relative energies between the axial, and the equatorial conformers. Interestingly, all equatorial (2)PXZ derivatives are sensibly more stable than the axial ones while both axial and equatorial (2)PTZ conformers are almost isoenergetic and will most likely coexist.

In Tables S3 (2) and S4 (S5), we have further compared ΔE_V^{ST} calculated for the equatorial (axial) conformers with the 6-31G(d,p) and the def2-

TZVP basis sets and we have found small differences between the two. On the basis of these results, we adopted the smallest 6-31G(d,p) basis set that considerably reduces the computational time when computing excited states properties, and in particular when searching for the energy minimum on the singlet and triplet excited states potential energy surfaces.

Furthermore, we perform some post-processing of the results in order to determine quantitatively the nature of the calculated excited states. Previously, we have stressed the importance of referring to Natural Transition Orbitals (NTOs) when analyzing the reorganization of the electronic density upon electronic transition to the excited states.[32] To characterize the spatial separation of the frontier orbitals, we have introduced a metric based on the hole and electron distance Δr, inversely proportional to the experimentally measured and/or calculated ΔE^{ST} values. In a recent attempt to classify compounds for OLED applications, Chen et al[53] have established, in addition to Δr, a metric I based on the absolute value of the Highest Occupied NTO (HONTO) and the Lowest Unoccupied NTO (LUNTO) overlap, similar to the Λ metric developed by Tozer and co.[47,54] They found that compounds with small I for both S_1 (I_S) and T_1 (I_T) and large Δr_S and Δr_T, compatible with S_1 and T_1 bearing an large CT character, are conditions to minimize their ΔE^{ST} values. Here, we rely on the more compact attachment/detachment formalism.[55,56] Indeed, in this approach, the difference density matrix between the ground and an excited state is diagonalized to obtain the occupation numbers (eigenvectors) and orbitals (eigenvalues) for each electronic transition selected. The detachment (attachment) density matrix are obtained by summing up over up the eigenvectors possessing negative (positive) occupations, weighted by the absolute value of their occu-

pations. Instead of referring to HONTO and LUNTO orbitals, in the attachment/detachment approach it is possible to directly access to the localization of the electron density of the ground state that is removed upon electronic excitation (i.e. the detachment density matrix) and rearranged in the excited state (i.e. the attachment density) by considering all the orbitals characteristic of the electronic transitions. The attachment and detachment densities are often seen as the hole and electron densities, respectively. From those, we have computed two metrics to identify and quantify CT excited-states, namely the averaged Δr [57] and ϕ_S [58,59] the overlap between the attachment and detachment density matrices. Both metrics are computed using the NANCY_EX package.[58,59] and allow us to unambigously determine the nature of the excited states being either ICT or LE.

3   Results and discussion

3.1   Equatorial conformers

3.1.1   Frontier orbitals characterization

We first start by investigating the shape and energy of the frontier orbitals of the different D-A and D-A-D equatorial conformers (i.e. with a D-A dihedral angle of about 90 degrees) and of their constituting D and A units (see Figure 2 and Figures S1 to S5). Among the two donors initially investigated, PXZ appears to have a slightly stronger donor character than PTZ as well as a larger band gap. We also observe that TDZ has the strongest acceptor character, followed by OXD and TAZ. The almost perpendicular arrangement of D and A aromatic planes with respect to each other (see Table S6) guarantees a good spatial separation of the respective frontier orbitals at the expense of a weak orbital overlap. We note that the HOMO and (H-1)OMO levels of D-A-D compounds are (nearly) degenerated

due to the high symmetry that is retained throughout the optimization of the geometries (see Table 1 for the symmetry point groups at the optimized equatorial geometry). The HOMO and (H-1)OMO orbital shapes are quite similar being the anti-bonding and the bonding linear combination of the HOMO of PXZ or PTZ. When comparing their HOMO energies, we observe almost no change in energy (in agreement with the experiment,[31] see Figure S6) and orbital shapes when comparing PXZ or PTZ and their corresponding D-A and D-A-D compounds, highlighting the weak electronic interaction between the HOMOs of D and A. Conversely, despite exhibiting similar or larger LUMO energy separation, the D-A and D-A-D LUMOs appear to be around 0.2 and 0.4 eV stabilized with respect to the LUMO level of the acceptors, emphasizing the higher electronic interaction between the LUMOs of the D and the A units. Therefore, a decrease in the energy band gap is observed when going from D-A to D-A-D molecules. Based on these frontier orbitals diagrams (see Figure 2 and Figures S1 to S5), in a first approximation the bluest compounds are obtained for D-A with TAZ acceptor, due to the higher-lying LUMO orbital of this unit.

3.1.2 Excited States Calculations and Characterization

Not surprisingly, the TDA calculations confirm that S_1 and T_1 states of D-A-D molecules are red-shifted with respect to the D-A ones and that the bluest compounds are obtained when a TAZ acceptor is considered (see Table S3). We also mention that correct color ordering, *i.e.*, theoretically determined relative energies for absorption, agree with the ordering experimentally found for the compounds actually synthesized (2PXZ-OXD, 2PXZ-TAZ and 2PXZ-TAZ).[30,31] Among the proposed new molecules, 2PTZ-TAZ appears to be even bluer than the sky-blue 2PXZ-TAZ compound (S_1 energy is roughly

0.3 eV higher in energy, see Table S3). In great contrast with the experiments, the whole set of compounds exhibit vanishing oscillator strengths ($O.S.$) for their lowest singlet excited states. Previous theoretical estimates[30] at the CAM-B3LYP/cc-pVDZ level reported similar negligible values for all cases studied (PXZ-OXD, PXZ-TAZ, 2PXZ-OXD, and 2PXZ-TAZ). We are also aware that the TDA causes the oscillator strengths to incur in some error,[60] since the f-sum rule, also known as the Thomas-Reiche-Kuhn sum rule, is no longer fulfilled exactly. However, we have carefully checked this point by rerunning some calculations at the full TD-DFT level, without noticing significant changes in the O.S. values. We have also carefully controlled that the low oscillator strengths of S_1 excitations are not due to symmetry-forbidden transitions but are a consequence of the large twist angle between D and A units, which offers a poor overlap between the frontier orbitals. Moreover, the magnitude of the oscillator strengths of the S_1 transitions does not increase even when considering geometry relaxation towards the energy minimum of S_1 potential energy surface. Indeed, in the excited state, we note a further increase of D-A torsion angles (even closer to 90 degrees, see Table S6) irrespective of the donor and the acceptor, which is characteristic of a Twisted Intramolecular Charge Transfer (TICT) state.[61]

In their classification, Chen et al.[53] distinguished three types of materials depending on the extent of the separation Δr between the HONTO and LUNTO centroids as well as the overlap I between these two NTOs for both S_1 and T_1. For efficient TADF materials, both Δr_S and Δr_T must be large, as well as I_S and I_T must be small. Here, we characterize the excited properties of the different molecules using Δr calculated in terms of the attachment/detachment formalism, with ϕ_S the overlap between the corresponding densities. Typically, a Δr larger than 1.5-2.0 Å has been

proposed before to identify a CT excitation,[57] while ϕ_S amounts to 0 (1) when the electronic transition bears an charge-transfer character (is [LE]) by nature. Intermediate values describe excitations exhibiting a mixed CT-LE character with either dominant CT or LE character depending if ϕ_S is smaller or larger than 0.5, respectively.

All the D-A molecules display a similar electronic structure with T_2 lying above T_1 and S_1 while for D-A-D ones, S_1 and S_2 are lying above T_1 and T_2 and below T_3 and T_4. The presence of two singlet states close in energy certainly explains the broader absorption profiles observed experimentally for D-A-D compounds with respect to D-A molecules.[29] Indeed, each bright state can come up with its own absorption broadening, summing up which results in a wider absorption band. To characterize the nature of those states, in Table 1 we have reported for PXZ-OXD and PTZ-TAZ the Δr values corresponding to S_1 and observed that they are largely above the commonly adopted threshold to characterize CT-like transition, with values ranging from 4.0 to 6.5 Å. In addition, ϕ_S values for these states are all below 0.5 which allows us to establish that the electronic transitions to S_1 have a dominant CT character. PXZ-OXD, which is representative of all D-A compounds studied here at the exception of PTZ-TAZ, exhibits a T_1 (T_2) state with a marked as CT-like (LE) character with Δr largely above 2.0 Å (close to 0 Å) and ϕ_S close to 0 (1). In a NTO analysis, S_1, T_1 and T_2 excitations appear to be also in this case dominated by a HONTO to LUNTO excitations (see Table S7).

We further confirm the nature of these transitions (CT-like for S_1 and T_1 and LE-like for T_2) by inspecting their respective attachment/detachment electronic densities (see Figure 3 left panel for example, for PXZ-OXD). Typically, CT (LE) transitions involve a large (small) electronic reorganization

14

of the density from the donor to acceptor unit. As suggested by Δr and ϕ_S values, the triplet states of PTZ-TAZ exhibit an opposite nature with respect to PXZ-OXD, namely S_0-T_1 and S_0-T_2 transitions are LE- and CT-like, respectively, while S_0-S_1 keeps its CT-character (see Figure 3 right panel). The hole and the electron densities of S_0-T_1 excitation are mainly localized on the PTZ units, similarly to Type I compounds described by Milián-Medina and Gierschner[26] for which the electronic interaction between D and A units is extremely weak.

A qualitative estimate of the singlet (triplet) D-A electronic couplings is given in a state representation by the energy splitting between the S_1 (T_1) states of D and A units, assuming that the resulting S_1 (T_1) state of the D-A molecule is mainly determined by a bonding combination of S_1 (T_1) states of D and A moieties. Here, one can guess the evolution of the electronic coupling by considering the energy stabilization of the S_1 (T_1) state with respect to S_1 (T_1) states of the D and A units. In Figures 4 and S7 to S10, we have used such a representation for the lowest singlet and triplet excited states of the individual D and A units, as well as for the combinations D-A and D-A-D. The stabilization in energy of T_1 states of D-A compounds is the lowest for PTZ-TAZ, confirming that the electronic interaction between the T_1 states of the D and A units is the weakest for this compound among all. The choice of the donor moiety is crucial since the PTZ donor tends to reduce D-A electronic interactions, an effect which is attributed to a bigger deviation from planarity for PTZ with respect to PXZ (see Figure S11). The non-planarity of the TAZ acceptor (see Figure S12) further contributes to the reduced D-A electronic interactions, in line with the lowest triplet stabilization energy and the largest $\phi_S(T_1)$ values observed for PXZ-TAZ and PTZ-TAZ (see Table S3). Hence, depending on the respective conformation

Journal of Materials Chemistry C Accepted Manuscript

of the donor and the acceptor, it is possible to induce at will either a LE or a CT character to T_1. We note that the stabilization of S_1 states in the D-A structure with respect to the isolated PTZ and TAZ is not affected by the lack of planarity. Indeed, in constrast with singlet excited states, triplets are subject to the exchange energy which increases their spatial confinement and enhances their LE character.[62,63]

Concerning D-A-D compounds, all of them, with the exception of 2PXZ-OXD and 2PTZ-OXD, have Δr values close to 0 Å for all excited states transitions (see Tables 1 and S3) as expected for symmetric molecules.[59] This is not necessarily an indication of LE character, but a mathematical limitation of the Δr metrics, that may hide the true nature of the excited states of D-A-D highly symmetric compounds.[59] For 2PXZ-OXD and 2PTZ-OXD, Δr for T_1, T_2, S_1 and S_2 ranges between 1.7 and 1.8 Å because of the V-shape of the OXD acceptor (see Figure S13) which points to a dependence of Δr on detailed geometrical aspects. Similarly to D-A compounds, the lowest triplet states of D-A-D molecules bear a strong CT character, with the exception of 2PTZ-TAZ for which a weaker CT character is observed (see Table 1 and S3). Grafting an additional donor to PTZ-TAZ does not further stabilize the T_1 state, however, allows for the electron density to further delocalize on the acceptor unit (see Figure 5 right panel) compared to its corresponding D-A compound (see Figure 3 right panel). This rises the CT character of T_1, confirmed by the decrease of $\phi_S(T_1)$ compared to PTZ-TAZ. In this particular case, the simplified HONTO to LUNTO representation (see Table S7) of the different excitations is not appropriate for the description of all excited states and one should invoke the contribution of other pairs of NTOs to complement it. A representation of the different electronic transitions in terms of attachment/detachment electronic densities is

16

therefore more pertinent at increasing complexity of the molecular structure. Finally, analogously to D-A molecules, relaxed S_1 states of all studied D-A-D compounds present vanishing oscillator strengths (similarly to S_1 transitions obtained from vertical excitations) due to their TICT character.

3.1.3 Singlet-Triplet gap calculations

Low values for the vertical ΔE_V^{ST} are always obtained, ranging from 0.01 to 0.17 eV for D-A and from 0.01 to 0.1 eV for D-A-D. As expected going from D-A structures to D-A-D materials results to a slight decrease in ΔE_V^{ST} values due to higher stabilization of the S_1 and T_1 states. The largest ΔE_V^{ST} are obtained for PTZ-TAZ and 2PTZ-TAZ in line with their largest $\phi_S(T_1)$ value, *i.e.* their weaker CT character. In this case, the exchange interaction energy is more effective in stabilizing the triplet states and therefore increases the singlet-triplet gap.[62] Still, overall, ΔE_V^{ST} is reduced when going from PTZ-TAZ to 2PTZ-TAZ essentially because the T_1 CT character is increased. In such a case where T_1 holds a LE character, the addition of a second D moiety appears as an interesting design strategy to bring some CT character to T_1 and to subsequently reduce ΔE_V^{ST}. We have also evaluated the geometry relaxation of both T_1 and S_1 states for D-A and D-A-D compounds and did not notice major changes in terms of ΔE_A^{ST} compared to ΔE_V^{ST} for both D-A and D-A-D materials. Interestingly, on one hand, all λ_{S_1} and λ_{T_1} of OXD- and TDZ-based compounds appear to be very similar (see table 3) most likely to their similar chemical structures and the planar structure of the electron acceptor. On the other hand, TAZ-based compounds exhibit λ_{S_1} and λ_{T_1} that are larger because of the non-planar structure of this electron acceptor. We also see that PXZ-based compounds have overall smaller relaxation energies than PTZ ones, which is consistent with a smaller

geometrical reorganization towards a planar conformation of the PXZ unit compared to PTZ. Similarly to reorganization energy in charge transport, the more extended D-A-D compounds exhibit smaller λ_{S_1} and λ_{T_1} than D-A ones because of overall smaller variations in molecular degrees of freedom (bonds, angles, dihedral) compared to the ground-state geometry. Finally, the ΔE_A^{ST} adiabatic values always remain positive in contrast with the results obtained by Sun et *al.*[23] with PBE and B3LYP functionals.

We compare now our results for the set of molecules (i.e. 2PXZ-OXD, 2PXZ-TDZ and 2PXZ-TAZ) for which experimental ΔE^{ST} values (obtained from the blue edges of low-temperature fluorescence and phosphorescence spectra) are available.[30,31] Adachi *et al.* measured the singlet-triplet gap of 2PXZ-OXD,[30] 2PXZ-TDZ[31] and 2PXZ-TAZ[30] in doped films (0.15, 0.11 and 0.23 eV, respectively) which compare well with our theoretical estimates (0.01, 0.007 and 0.02 eV for ΔE_V^{ST}, see Table S3 and 0.008, 0.006 and 0.11 eV for ΔE_A^{ST}, see Table 3, respectively) leading to an error of only 0.1-0.2 eV. We will discuss further this discrepancy, just noting here that previously published values of ΔE_V^{ST} calculated at the CAM-B3LYP/cc-pVDZ level[30,31] are affected by a systematic error of 0.4-0.6 eV, in agreement with benchmark studies,[64] which is largely reduced in this work. Indeed, range-separated functionals (e.g. CAM-B3LYP) are generally not recommended for triplet states, due to orbital instabilities.[65]

3.2 Axial conformers

The evaluation of the torsion potential for the rotation about the D-A bond (see Figure 6) indicates that for PTZ derivatives axial conformers are just as stable as equatorials ones, contrarily to what happens for PXZ derivatives. Of course, axial derivatives show higher hybridization between

the frontier orbitals of donor and the three acceptors resulting in larger de-
localization of the HOMO and LUMO orbitals (see for example HOMO and
LUMO orbitals in Figures S14 and S15) over the whole D-A and D-A-D
compounds. Even if some ϕ_S values for S_1 are ranging from 0.64 to 0.95,
hence compatible with a mixed CT-LE to LE character, $\phi_S(T_1)$ values for
axial conformers lie in a really narrow range around 0.8, characteristic of a
dominant LE character, and accordingly quite large ΔE_V^{ST} values (above 0.6
eV) are obtained. In addition, because of the dominant LE character of the
lowest singlet and triplet excited states, the S_1 and T_1 energies are signifi-
cantly blue-shifted compared to the equatorial ones (cf Tables 1, 2 and S3).
As a consequence of a large torsional energy barrier (larger than 3 kcal/mol
in gas-phase, see Figure 6), one can expect to observe dual emission from the
LE and CT S_1 states of the axial and the equatorial conformers, respectively.
Even though the oscillator strengths of the axial conformers are much larger
than the equatorial ones, we foresee that most of the fluorescence collected
would arise from the equatorial conformer, because, in addition to prompt
fluorescence, TADF is expected to take place in equatorial-like conformers in
contrast with axial-like conformers.

Furthermore, due to larger band gap of the axial conformers, efficient
Förster energy transfer towards neighboring equatorial conformers could pos-
sibly happen. This mechanism was evidenced by Tanaka et al.[39] on a PTZ-
TRZ TADF emitter. The observed prompt fluorescence of the axial con-
former appears to be completely quenched when the temperature increases,
which is compatible with an increase in the rate of the energy transfer pro-
cess. In addition, the delayed fluorescence spectrum matches perfectly the
emission spectrum of the equatorial conformer highlighting the efficient up-
conversion of triplet excitons into singlets (resulting in OLEDs with EQE of

10.8 %) characteristic of an emitter exploiting a TADF mechanism. Combining all these elements together, the coexistence of two conformers does not appear to be a key limitation in order for a compound to work as an efficient TADF emitter.

3.3 Conformation influence on the oscillator strength and singlet-triplet splitting

We have so far demonstrated that both D-A and D-A-D systems could act as efficient TADF materials exhibiting extremely small singlet-triplet splitting gap. However, the oscillator strengths of these compounds are vanishing because of the pronounced CT character of their S_1 state. Interestingly, TADF emitters exhibit usually quite broad emission spectra which in general are associated with the conformational disorder due to their high molecular flexibility.[66] When focusing on the equatorial conformers the torsion energy profiles appear to be rather flat (see again Figure 6) suggesting the possibility of thermally-activated variations in the D-A torsion angle, of up to 45 degrees around the minimum of the potential energy surface. As expected, the ΔE_V^{ST} decreases when the D-A torsion angle is increased (see Figures 7 top left panel for PXZ-OXD and top right panel for PTZ-TAZ, respectively) which comes along with an increase of the CT character of the S_1 state in agreement with the decrease of $\phi_S(S_1)$ (see Figure 7 bottom left panel for PXZ-OXD and bottom right panel for PTZ-TAZ). Similarly, the CT character of the PXZ-OXD T_1 state increases ($\phi_S(T_1)$ decreases) when increasing the D-A torsion angle. Not surprisingly, for the equatorial conformer CT states are stabilized with respect to their corresponding LE states because of the twisted conformation. In great contrast to PXZ-OXD, $\phi_S(T_1)$ for PTZ-TAZ is almost constant (having a LE character) irrespective of the value of the dihedral angle between the PTZ donor and the TAZ acceptor, consis-

tently with its larger ΔE_V^{ST} compared to other D-A compounds. In addition, the oscillator strength increases significantly when going out of the equatorial minimum of the potential energy surface, since the overlap between the hole and electron densities (*i.e.* $\phi_S(S_1)$) increases. Actually, we have found that the oscillator strength exhibits a linear relation with $[\phi_S(S_1)]^2$ and does not thus deviate from its definition (see Figure S16). Light emission is then likely to be assisted by soft vibrational modes in these series of compounds, which could appear as a general feature of efficient TADF emitters. In Table 4, we have calculated the Boltzmann-averaged ΔE_V^{ST} and oscillator strengths for the PXZ- and PTZ-based D-A compounds and observed a sensible increase of both quantities compared to the values obtained for the optimized geometries in Table 1. In addition, we note that ΔE_V^{ST} standard deviations are as large as the average values, implying that different conformations will contribute preferentially either to the light emission or to the up-conversion of triplet excitons into singlet ones. Experimental inspection of the PL properties of 2PXZ-OXD and 2PXZ-TAZ molecules in solution reveals that in view of the reported[30] PLQY values, D-A-D molecules (i.e. 2PXZ-OXD and 2PXZ-TAZ) can emit more total (prompt and delayed) fluorescence than D-A ones. For D-A-D compounds, we have evaluated the torsion profiles of 2PXZ-OXD, 2PXZ-TDZ and 2PXZ-TAZ by varying both D-A torsion angles (ϕ_1 and ϕ_2) between 0 and 90 degrees resulting in two dimensional maps (see Figure S17) which confirmed that the equatorial geometries are the most stable for all 2PXZ D-A-D compounds considered here. In addition, ΔE^{ST} and oscillator strength are minimal at these geometries (see Figures S18 and S19, respectively) in agreement with an increase of the CT character with respect to the D-A compounds (see $\phi_S(S_1)$ and $\phi_S(T_1)$ maps in Figure S20 and S21, respectively).

Overall, moving away from the global (equatorial) minimum, we note an increase ΔE^{ST} for both D-A and D-A-D systems, followed by an increase in average $\phi_S(T_1)$ compared to a more modest for $\phi_S(S_1)$ which confers to T_1 a mixed CT-LE character, while S_1 remains a CT-like state and is much less affected by the torsional dynamics. The Boltzmann-averaged oscillator strength for the 2PXZ molecules is comparable to the oscillator strength calculated for PXZ compounds. This feature comes along with lower average ΔE_V^{ST} for 2PXZ derivatives, as well as lower standard deviations with respect to PXZ molecules. It appears to be linked to the relative insensivity of both ΔE_V^{ST} and the oscillator strength to the variation in torsion angle (ϕ_1 and ϕ_2) beyond 60 degrees (see Figures S18 and S19). The lower ΔE_V^{ST} standard deviations and the similar averaged oscillator strengths for 2PXZ molecules with respect to D-A systems suggest that, for the D-A-D compounds, a set of conformers with rather low ΔE_V^{ST} contributes both to the triplet-singlet interconversion and to light emission. These factors prompt us to hypothesize that in real devices D-A-D compounds could behave more efficiently than D-A ones.

4   Conclusions

We have carried out an in-depth theoretical study to characterize, and further engineer, a set of new TADF emitters based on combining adequate donor (PXZ, PTZ) and acceptor (OXD, TDZ, TAZ) chromophores following the D-A or D-A-D sequence. Since good candidates for TADF should possess spatially separated frontier orbitals, a feature directly related with a low singlet-triplet energy gap, we have explored this issue by relying on the attachement/detachment formalism simplifying the description of the excitations. Based on this formalism, we have calculated the electron-hole separa-

tion Δr and the overlap between the hole and electron densities ϕ_S associated with the excitation. Among the two indexes, ϕ_S appears to be the most reliable one for assigning the correct nature (CT or LE) of the lowest excited states for both non-symmetric D-A and symmetric D-A-D compounds. We have also found that for PXZ-based compounds, equatorial conformers are more stable than axial ones while for PTZ-based compounds, there is most likely a coexistence of equatorial and axial conformers because of the small energy difference between these conformers. Still, for both donors, the equatorial conformers are expected to contribute predominantly the RISC process since their singlet-triplet gap is much smaller. Indeed, their low ΔE^{ST} values are associated with lowest singlet and triplet transitions exhibiting a strong CT character and thus ϕ_S values close to 0.

We have also identified that connecting donor and acceptor units in a twisted conformation (*i.e.* equatorial conformation) is a necessary condition but not sufficient for obtaining the spatial separation between the hole and electron densities associated with low ΔE^{ST} values. In terms of light-emitting properties, we have demonstrated that oscillator strengths for the series of compounds studied here are vanishing in the equatorial conformations at their optimized ground and first singlet excited state geometries. However, the torsional potential of all these compounds is flat enough to make them able, even at room temperature, to access to a set of conformations displaying non-negligible oscillator strengths, hence light emission appears to be a vibrationally assisted process in these compounds. In addition, we have rationalized the experimental observation that D-A-D compounds emit more light than D-A ones, since: (a) ΔE^{ST} average (over the different configurations considered) and corresponding standard deviations are smaller for D-A-D molecules, and (b) averaged oscillator strengths are still comparable.

The overall superior TADF properties of D-A-D systems appears to be a consequence of the largest number of donor units connected to the central acceptor with a considerable number of D-A-D conformations to participate to the interconversion between triplet and singlet excitons as well as the light emission, which is not the case for D-A compounds.

Acknowledgements

Associated contents

The Supporting Information contains: (i) isocontour plots of the calculated frontier orbitals (HOMO and LUMO), (ii) excited states diagrams for all the monomers (PXZ, OXZ, TAZ, PTZ, TDZ) and the corresponding D-A and D-A-D combinations studied, (iii) plots of the oscillator strengths normalized to the S_1 transition energy as a function of $[\phi_S(S_1)]^2$ and (iv) torsion energy profiles, ΔE^{ST}, $\phi_S(S_1)$ and $\phi_S(T_1)$ as a function of the torsion angles between the acceptor units (OXD, TDZ and TAZ) with the two PXZ donors for 2PXZ-OXD, 2PXZ-TDZ and 2PXZ-TAZ, tables reporting (iv) the relative energies between the axial and the equatorial conformers, (v) tables with S_1, T_1 energies and their associated ϕ_S and Δr values as well as the oscillator strengths for both axial and equatorial conformers, (vi) equilibrium D-A torsion angle for the optimized ground-state, S_1 and T_1 geometries and (vii) NTO representation of the excited states of equatorial compounds.

References

[1] K. Müllen and U. Scherf, *Organic Light-Emitting Devices*, 2006.

[2] A. Endo, K. Sato, K. Yoshimura, T. Kai, A. Kawada, H. Miyazaki and C. Adachi, *Appl. Phys. Lett.*, 2011, **98**, 083302.

[3] T. Nakagawa, S.-Y. Ku, K.-T. Wong and C. Adachi, *Chem. Commun.*, 2012, **48**, 9580–9582.

[4] Q. Zhang, J. Li, K. Shizu, S. Huang, S. Hirata, H. Miyazaki and C. Adachi, *J. Am. Chem. Soc.*, 2012, **134**, 14706–14709.

[5] H. Uoyama, K. Goushi, K. Shizu, H. Nomura and C. Adachi, *Nature*, 2012, **492**, 234–238.

Journal of Materials Chemistry C Accepted Manuscript

[6] K. Sato, K. Shizu, K. Yoshimura, A. Kawada, H. Miyazaki and C. Adachi, *Phys. Rev. Lett.*, 2013, **110**, 247401.

[7] H. Yersin, A. Rausch, R. Czerwieniec, T. Hofbeck and T. Fischer, *Coord. Chem. Rev.*, 2011, **255**, 2622–2652.

[8] C. Brown and D. Kondakov, *J Soc Inf Disp.*, 2004, **12**, 323–327.

[9] A. Endo, M. Ogasawara, A. Takahashi, D. Yokoyama, Y. Kato and C. Adachi, *Adv. Mater.*, 2009, **21**, 4802–4806.

[10] K. Goushi, K. Yoshida, K. Sato and C. Adachi, *Nat. Photonics*, 2012, **6**, 253–258.

[11] T. Serevičius, T. Nakagawa, M.-C. Kuo, S.-H. Cheng, K.-T. Wong, C.-H. Chang, R. Kwong, S. Xia and C. Adachi, *Phys. Chem. Chem. Phys.*, 2013, **15**, 15850–15855.

[12] K. Udagawa, H. Sasabe, C. Cai and J. Kido, *Adv. Mater.*, 2014, **26**, 5062–5066.

[13] Q. Wang, I. Oswald, X. Yang, G. Zhou, H. Jia, Q. Qiao, Y. Chen, J. Hoshikawa-Halbert and B. Gnade, *Adv. Mater.*, 2014, **26**, 8107–8113.

[14] Y. Tao, K. Yuan, T. Chen, P. Xu, H. Li, R. Chen, C. Zheng, L. Zhang and W. Huang, *Adv. Mater.*, 2014, **26**, 7931–7958.

[15] K. Shizu, H. Tanaka, M. Uejima, T. Sato, K. Tanaka, H. Kaji and C. Adachi, *J. Phys. Chem. C*, 2015, **119**, 1291–1297.

[16] Q. Zhang, B. Li, S. Huang, H. Nomura, H. Tanaka and C. Adachi, *Nat. Photonics*, 2014, **8**, 326–332.

[17] R. Nobuyasu, Z. Ren, G. Griffiths, A. Batsanov, P. Data, S. Yan, A. Monkman, M. Bryce and F. Dias, *Adv. Opt. Mater.*, 2016, **4**, 648–653.

[18] P. L. Santos, J. S. Ward, P. Data, A. S. Batsanov, M. R. Bryce, F. B. Dias and A. P. Monkman, *J. Mater. Chem. C*, 2016, **4**, 3815–3824.

[19] J. Gibson, A. P. Monkman and T. J. Penfold, *ChemPhysChem*, 2016, **17**, 2956–2961.

[20] T. Ogiwara, Y. Wakikawa and T. Ikoma, *J. Phys. Chem. A*, 2015, **119**, 3415–3418.

[21] S. Huang, Q. Zhang, Y. Shiota, T. Nakagawa, K. Kuwabara, K. Yoshizawa and C. Adachi, *J. Chem. Theory Comput.*, 2013, **9**, 3872–3877.

[22] T. Penfold, *J. Phys. Chem. C*, 2015, **119**, 13535–13544.

[23] H. Sun, C. Zhong and J.-L. Brédas, *J. Chem. Theory Comput.*, 2015, **11**, 3851–3858.

[24] Y. Shu and B. Levine, *J. Chem. Phys.*, 2015, **142**, 104104.

[25] R. Gomez-Bombarelli, J. Aguilera-Iparraguirre, T. D. Hirzel, D. Duvenaud, D. Maclaurin, M. A. Blood-Forsythe, H. S. Chae, M. Einzinger, D.-G. Ha, T. Wu, G. Markopoulos, S. Jeon, H. Kang, H. Miyazaki, M. Numata, S. Kim, W. Huang, S. I. Hong, M. Baldo, R. P. Adams and A. Aspuru-Guzik, *Nat. Mater.*, 2016, **15**, 1120–1127.

[26] B. Milián-Medina and J. Gierschner, *Org. Electron.*, 2012, **13**, 985–991.

[27] S. Hirata, Y. Sakai, K. Masui, H. Tanaka, S. Lee, H. Nomura, N. Nakamura, M. Yasumatsu, H. Nakanotani, Q. Zhang, K. Shizu, H. Miyazaki and C. Adachi, *Nat. Mater.*, 2015, **14**, 330–336.

Journal of Materials Chemistry C Accepted Manuscript

[28] M. Kim, S. Jeon, S.-H. Hwang and J. Lee, *Adv. Mater.*, 2015, **27**, 2515–2520.

[29] H. Tanaka, K. Shizu, H. Nakanotani and C. Adachi, *Chem. Mater.*, 2013, **25**, 3766–3771.

[30] J. Lee, K. Shizu, H. Tanaka, H. Nomura, T. Yasuda and C. Adachi, *J. Mater. Chem. C*, 2013, **1**, 4599–4604.

[31] H. Tanaka, K. Shizu, J. Lee and C. Adachi, *J. Phys. Chem. C*, 2015, **119**, 2948–2955.

[32] M. Moral, L. Muccioli, W.-J. Son, Y. Olivier and J. Sancho-García, *J. Chem. Theory Comput.*, 2015, **11**, 168–177.

[33] H. Tian, X. Yang, R. Chen, Y. Pan, L. Li, A. Hagfeldt and L. Sun, *Chem. Commun.*, 2007, 3741–3743.

[34] S. Agrawal, M. Pastore, G. Marotta, M. A. Reddy, M. Chandrasekharam and F. D. Angelis, *J. Phys. Chem. C*, 2013, **117**, 9613–9622.

[35] W. Zhou, Y. Wen, L. Ma, Y. Liu and X. Zhan, *Macromolecules*, 2012, **45**, 4115–4121.

[36] B. Kim, J. Lee, Y. Park, C. Lee and J. Park, *J. Nanosci. Nanotechnol.*, 2014, **14**, 6404–6408.

[37] S. Elkassih, P. Sista, H. Magurudeniya, A. Papadimitratos, A. Zakhidov, M. Biewer and M. Stefan, *Macromol. Chem. Phys.*, 2013, **214**, 572–577.

[38] K. Kamtekar, K. Dahms, A. Batsanov, V. Jankus, H. Vaughan, A. Monkman and M. Bryce, *J. Polym. Sci., Part A: Polym. Chem.*, 2011, **49**, 1129–1137.

[39] H. Tanaka, K. Shizu, H. Nakanotani and C. Adachi, *J. Phys. Chem. C*, 2014, **118**, 15985–15994.

[40] J. Perdew, M. Ernzerhof and K. Burke, *J. Chem. Phys.*, 1996, **105**, 9982–9985.

[41] C. Adamo and V. Barone, *J. Chem. Phys.*, 1999, **110**, 6158–6170.

[42] A. Becke and E. Johnson, *J. Chem. Phys.*, 2005, **123**, 154101.

[43] S. Grimme, J. Antony, S. Ehrlich and H. Krieg, *J. Chem. Phys.*, 2010, **132**, 154104.

[44] S. Grimme, S. Ehrlich and L. Goerigk, *J. Comput. Chem.*, 2011, **32**, 1456–1465.

[45] S. Hirata and M. Head-Gordon, *Chem. Phys. Lett.*, 1999, **314**, 291–299.

[46] M. Peach, M. Williamson and D. Tozer, *J. Chem. Theory Comput.*, 2011, **7**, 3578–3585.

[47] M. Peach and D. Tozer, *J. Phys. Chem. A*, 2012, **116**, 9783–9789.

[48] M. Peach, N. Warner and D. Tozer, *Mol. Phys.*, 2013, **111**, 1271–1274.

[49] J. Tomasi, B. Mennucci and R. Cammi, *Chem. Rev.*, 2005, **105**, 2999–3093.

[50] G. Scalmani and M. Frisch, *J. Chem. Phys.*, 2010, **132**, 114110.

[51] M. J. Frisch, G. W. Trucks, H. B. Schlegel, G. E. Scuseria, M. A. Robb, J. R. Cheeseman, G. Scalmani, V. Barone, B. Mennucci, G. A. Petersson, H. Nakatsuji, M. Caricato, X. Li, H. P. Hratchian, A. F. Izmaylov, J. Bloino, G. Zheng, J. L. Sonnenberg, M. Hada, M. Ehara, K. Toyota,

Journal of Materials Chemistry C Accepted Manuscript

R. Fukuda, J. Hasegawa, M. Ishida, T. Nakajima, Y. Honda, O. Kitao, H. Nakai, T. Vreven, J. A. Montgomery, Jr., J. E. Peralta, F. Ogliaro, M. Bearpark, J. J. Heyd, E. Brothers, K. N. Kudin, V. N. Staroverov, R. Kobayashi, J. Normand, K. Raghavachari, A. Rendell, J. C. Burant, S. S. Iyengar, J. Tomasi, M. Cossi, N. Rega, J. M. Millam, M. Klene, J. E. Knox, J. B. Cross, V. Bakken, C. Adamo, J. Jaramillo, R. Gomperts, R. E. Stratmann, O. Yazyev, A. J. Austin, R. Cammi, C. Pomelli, J. W. Ochterski, R. L. Martin, K. Morokuma, V. G. Zakrzewski, G. A. Voth, P. Salvador, J. J. Dannenberg, S. Dapprich, A. D. Daniels, Farkas, J. B. Foresman, J. V. Ortiz, J. Cioslowski and D. J. Fox, *Gaussian09 Revision A.01*, Gaussian Inc. Wallingford CT 2009.

[52] F. Weigend and R. Ahlrichs, *Phys. Chem. Chem. Phys.*, 2005, **7**, 3297–3305.

[53] T. Chen, L. Zheng, J. Yuan, Z. An, R. Chen, Y. Tao, H. Li, X. Xie and W. Huang, *Sci. Rep.*, 2015, **5**, 10923.

[54] M. Peach, P. Benfield, T. Helgaker and D. Tozer, *J. Chem. Phys.*, 2008, **128**, 044118.

[55] M. Head-Gordon, A. M. Grana, D. Maurice and C. A. White, *J. Phys. Chem.*, 1995, **99**, 14261–14270.

[56] A. Dreuw and M. Head-Gordon, *Chem. Rev.*, 2005, **105**, 4009–4037.

[57] C. Guido, P. Cortona, B. Mennucci and C. Adamo, *J. Chem. Theory Comput.*, 2013, **9**, 3118–3126.

[58] T. Etienne, X. Assfeld and A. Monari, *J. Chem. Theory Comput.*, 2014, **10**, 3896–3905.

[59] T. Etienne, X. Assfeld and A. Monari, *J. Chem. Theory Comput.*, 2014, **10**, 3906–3914.

[60] M. Grüning, A. Marini and X. Gonze, *Nano Lett.*, 2009, **9**, 2820–2824.

[61] Z. Grabowski, K. Rotkiewicz and W. Rettig, *Chem. Rev.*, 2003, **103**, 3899–4031.

[62] A. Köhler and D. Beljonne, *Adv. Funct. Mater.*, 2004, **14**, 11–18.

[63] A. Köhler and H. Bässler, *Mat. Sci. Eng. R.*, 2009, **66**, 71–109.

[64] D. Jacquemin, E. Perpète, I. Ciofini and C. Adamo, *J. Comput. Chem.*, 2008, **29**, 921–925.

[65] J. Sears, T. Koerzdoerfer, C.-R. Zhang and J.-L. Brédas, *J. Chem. Phys.*, 2011, **135**, 151103.

[66] M. Moral, W.-J. Son, J. Sancho-García, Y. Olivier and L. Muccioli, *J. Chem. Theory Comput.*, 2015, **11**, 3383–3392.

Journal of Materials Chemistry C Accepted Manuscript

Table 1: Calculated excited states energy values (E), oscillator strengths (O.S.[a]), ϕ_S, Δr as well as the dominant character of these transitions for the equatorial 2PXZ-OXD and 2PTZ-TAZ conformers. In bold, the corresponding S_1-T_1 energy difference.

	PXZ-OXD (C_s)					PTZ-TAZ (C_1)				
State	E (eV)	O.S.	ϕ_S	Δr (Å)	CT/LE	E (eV)	O.S.	ϕ_S	Δr (Å)	CT/LE
T_1	2.593	-	0.15	5.58	CT	3.177	-	0.72	0.85	LE
S_1	2.604	0	0.15	5.62	CT	3.345	4×10^{-4}	0.23	4.98	CT
T_2	3.037	-	0.79	0.12	LE	3.371	-	0.44	4.26	CT
ΔE^{ST}	**0.011**					**0.168**				
	2PXZ-OXD (C_s)					2PTZ-TAZ (C_2)				
State	E (eV)	O.S.	ϕ_S	Δr (Å)	CT/LE	E (eV)	O.S.	ϕ_S	Δr (Å)	CT/LE
T_1	2.478	-	0.16	1.85	CT	3.165	-	0.64	0.46	CT-LE
T_2	2.478	-	0.16	1.85	CT	3.165	-	0.64	0.46	CT-LE
S_1	2.939	0	0.17	5.75	CT	3.266	0	0.22	0.93	CT
S_2	2.488	0	0.15	1.86	CT	3.267	3×10^{-4}	0.22	0.93	CT
T_3	3.021	-	0.78	0.01	LE	3.311	-	0.51	0.67	CT-LE
T_4	3.021	-	0.78	0.01	LE	3.312	-	0.51	0.67	CT-LE
ΔE^{ST}	**0.010**					**0.101**				

[a] Note that the oscillator strengths are only defined for singlet excitations.

Table 2: Calculated excited states energy values (E), oscillator strengths (O.S.[a]), ϕ_S and Δr for the whole set of axial conformers. In bold, the corresponding S_1-T_1 energy difference.

	PXZ-OXD			PXZ-TDZ			PXZ-TAZ		
State	E (eV)	O.S.	ϕ_S	E (eV)	O.S.	ϕ_S	E (eV)	O.S.	ϕ_S
T_1	2.885	-	0.81	2.587	-	0.82	3.222	-	0.79
S_1	3.638	1.16	0.66	3.318	1.22	0.64	3.91	0.93	0.95
ΔE^{ST}	**0.754**			**0.731**			**0.687**		
	PTZ-OXD			PTZ-TDZ			PTZ-TAZ		
State	E (eV)	O.S.	ϕ_S	E (eV)	O.S.	ϕ_S	E (eV)	O.S.	ϕ_S
T_1	2.883	-	0.82	2.592	-	0.80	3.214	-	0.83
S_1	3.660	1.22	0.68	3.361	1.30	0.67	3.892	0.91	0.64
ΔE^{ST}	**0.777**			**0.769**			**0.678**		
	2PXZ-OXD			2PXZ-TDZ			2PXZ-TAZ		
State	E (eV)	O.S.	ϕ_S	E (eV)	O.S.	ϕ_S	E (eV)	O.S.	ϕ_S
T_1	2.810	-	0.81	2.522	-	0.79	3.148	-	0.82
S_1	3.515	1.75	0.72	3.226	1.84	0.69	3.786	1.44	0.82
ΔE^{ST}	**0.705**			**0.704**			**0.638**		
	2PTZ-OXD			2PTZ-TDZ			2PTZ-TAZ		
State	E (eV)	O.S.	ϕ_S	E (eV)	O.S.	ϕ_S	E (eV)	O.S.	ϕ_S
T_1	2.821	-	0.82	2.511	-	0.80	3.138	-	0.82
S_1	3.549	1.74	0.74	3.227	1.41	0.71	3.759	1.95	0.90
ΔE^{ST}	**0.728**			**0.716**			**0.622**		

[a] Note that the oscillator strengths are only defined for singlet excitations.

Table 3: Relaxation energies (λ_{rel}) and ΔE^{ST} calculated for the first singlet (S_1) and triplet (T_1) excited states.

	PXZ-OXD	PXZ-TDZ	PXZ-TAZ
λ_{S_1}(eV)	0.27	0.25	0.33
λ_{T_1}(eV)	0.27	0.24	0.37
ΔE^{ST}	**0.009**	**0.007**	**0.11**
	PTZ-OXD	PTZ-TDZ	PTZ-TAZ
λ_{S_1}(eV)	0.51	0.50	0.57
λ_{T_1}(eV)	0.50	0.49	0.53
ΔE^{ST}	**0.008**	**0.006**	**0.13**
	2PXZ-OXD	2PXZ-TDZ	2PXZ-TAZ
λ_{S_1}(eV)	0.19	0.20	0.24
λ_{T_1}(eV)	0.19	0.19	0.34
ΔE^{ST}	**0.008**	**0.006**	**0.11**
	2PTZ-OXD	2PTZ-TDZ	2PTZ-TAZ
λ_{S_1}(eV)	0.36	0.37	0.41
λ_{T_1}(eV)	0.35	0.36	0.32
ΔE^{ST}	**0.008**	**0.005**	**0.010**

Table 4: Boltzmann-averaged ΔE^{ST}, oscillator strengths and ϕ_S for S_1 and T_1 of D-A compounds and 2PXZ derivatives.

	PXZ-OXD	PXZ-TDZ	PXZ-TAZ
ΔE^{ST} (eV)	0.095 ± 0.102	0.076 ± 0.096	0.071 ± 0.065
O.S.	0.101 ± 0.152	0.094 ± 0.094	0.049 ± 0.046
$\phi_S(T_1)$	0.37 ± 0.11	0.32 ± 0.13	0.40 ± 0.13
$\phi_S(S_1)$	0.26 ± 0.08	0.26 ± 0.08	0.24 ± 0.07
	PTZ-OXD	PTZ-TDZ	PTZ-TAZ
ΔE^{ST} (eV)	0.055 ± 0.043	0.078 ± 0.054	0.183 ± 0.017
O.S.	0.025 ± 0.035	0.061 ± 0.061	0.022 ± 0.027
$\phi_S(T_1)$	0.41 ± 0.11	0.47 ± 0.07	0.73 ± 0.01
$\phi_S(S_1)$	0.21 ± 0.04	0.22 ± 0.05	0.26 ± 0.03
	2PXZ-OXD	2PXZ-TDZ	2PXZ-TAZ
ΔE^{ST} (eV)	0.061 ± 0.034	0.055 ± 0.036	0.057 ± 0.038
O.S.	0.081 ± 0.079	0.104 ± 0.101	0.049 ± 0.067
$\phi_S(T_1)$	0.39 ± 0.08	0.37 ± 0.09	0.40 ± 0.13
$\phi_S(S_1)$	0.23 ± 0.06	0.21 ± 0.06	0.21 ± 0.06
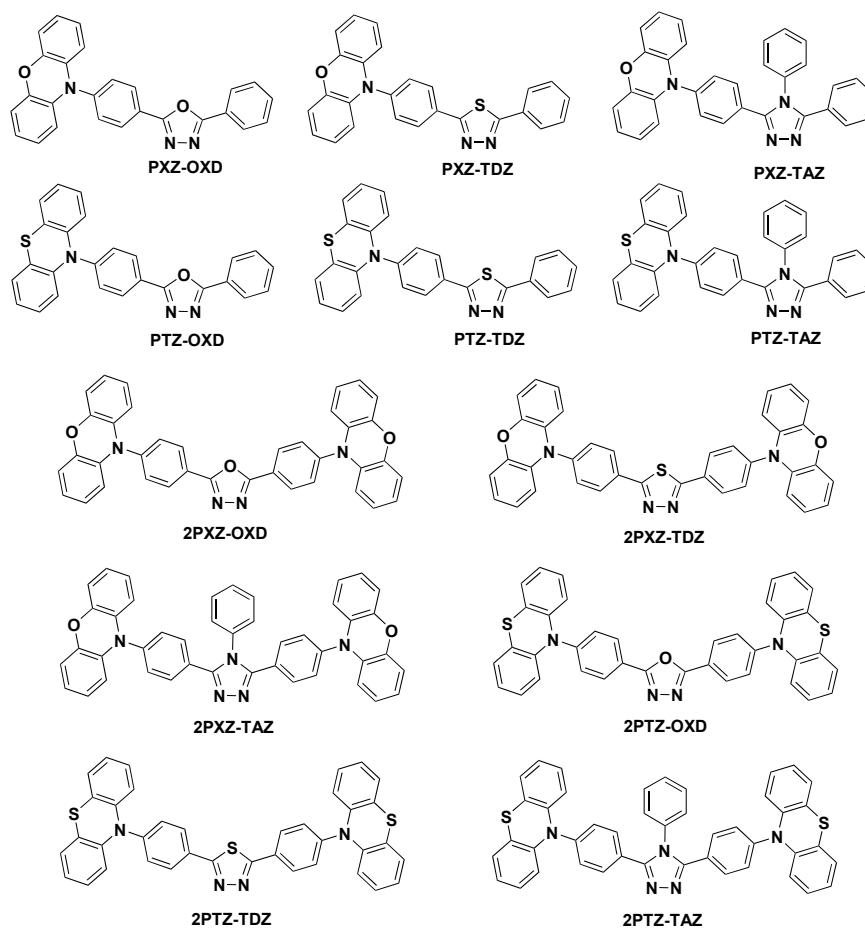
Figure 1: Chemical structures and shortened names of the investigated compounds. The hydrogen atoms and corresponding C–H bonds have been omitted for clarity.
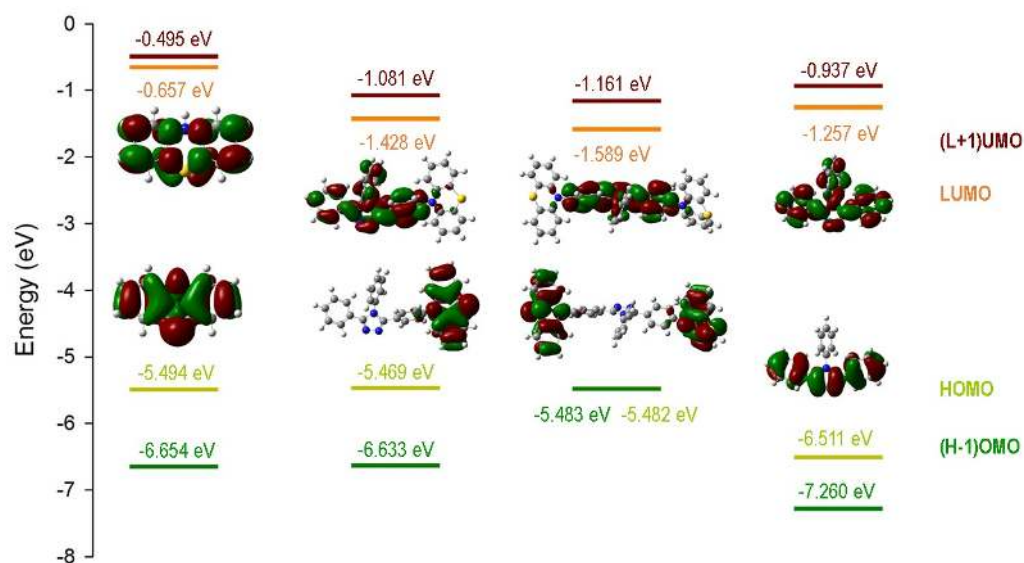
Figure 2: Isocontour plots (cutoff=0.02 a.u.) and energy of the frontier orbitals (HOMO and LUMO) calculated at the PBE0-D3(BJ)/6-31G(d,p) level of theory with the PCM module for solvent (toluene), for the case of combining PTZ (right) with TAZ (left) moieties giving rise to the PTZ-TAZ and 2PTZ-TAZ equatorial conformers (center). The size and color describe the amplitude and sign, respectively, of the lobes of orbitals.
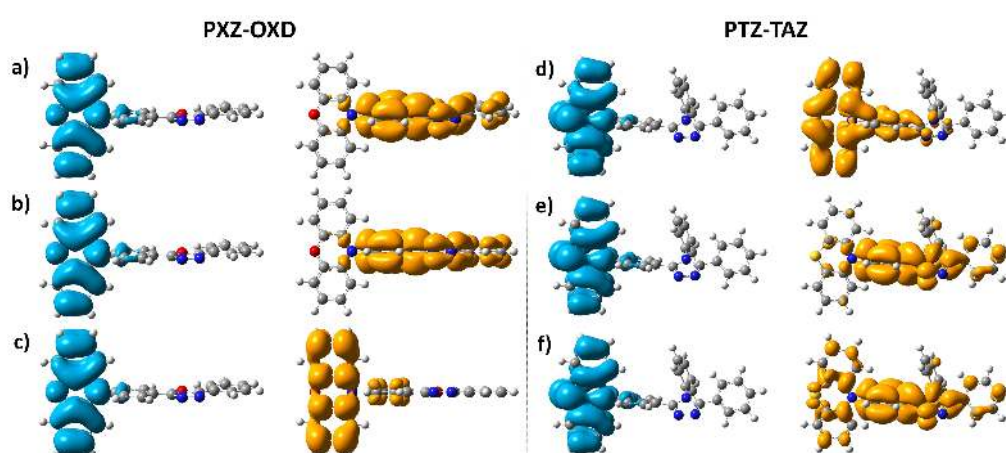
Figure 3: Hole (blue isocontour) and electron (orange isocontour) densities (cutoff=0.02 a.u.) obtained in the attachment/detachment formalism from TDA-PBE0-D3(BJ)/6-31G(d,p) calculations with the PCM module for solvent (toluene), for *(Left panel)* PXZ-OXD and *(Right panel)* PTZ-TAZ compounds associated with **a)** and **d)** T_1, **b)** and **e)** S_1 and, **c)** and **f)** T_2 excited states.
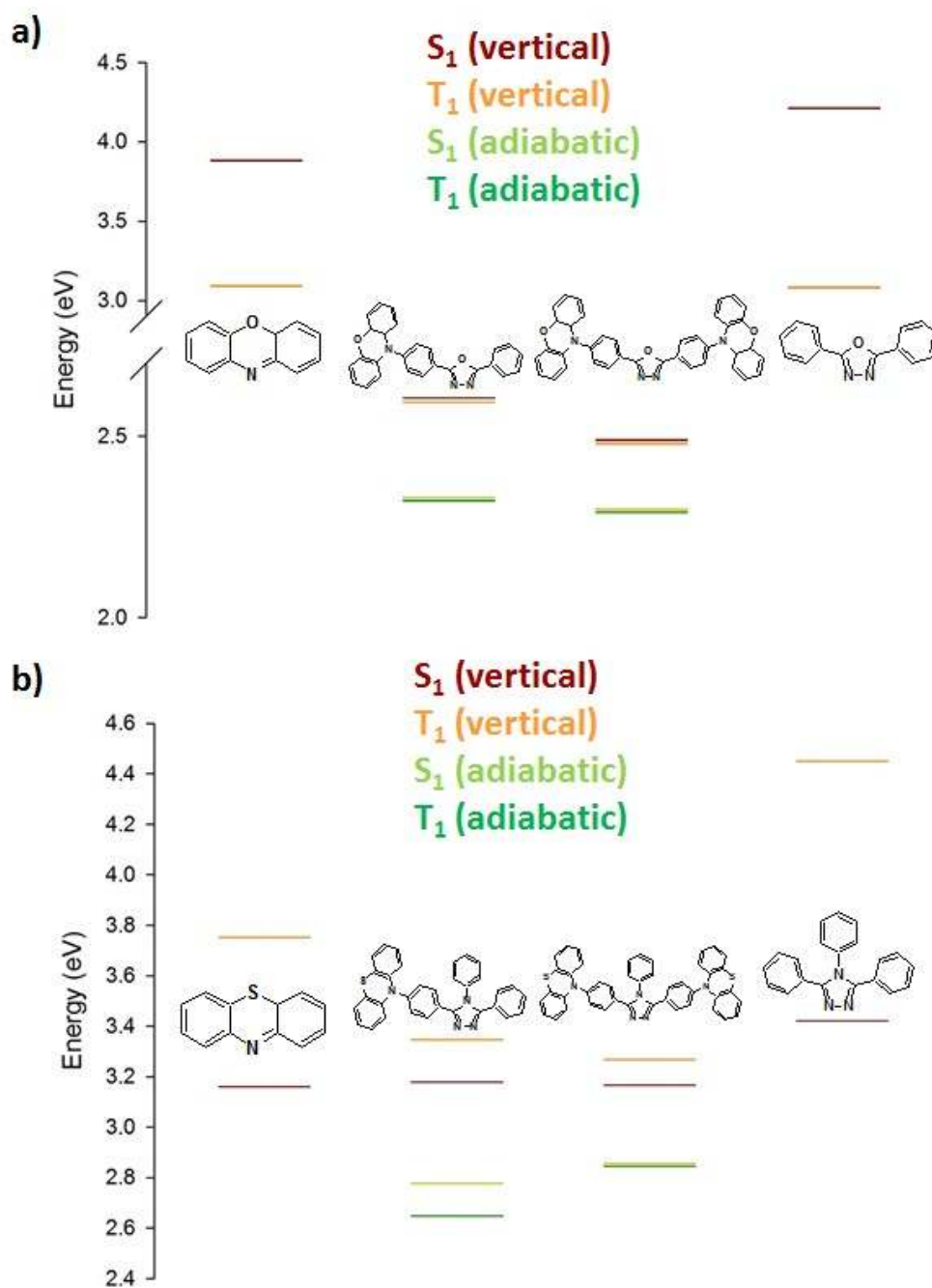
Figure 4: Excited states energy diagram for the case of combining PXZ (right) with OXD (left) moieties giving rise to the PXZ-OXD and 2PXZ-OXD equatorial conformers (center), as obtained from TDA-PBE0-D3(BJ)/6-31G(d,p) calculations with the PCM module for solvent (toluene).
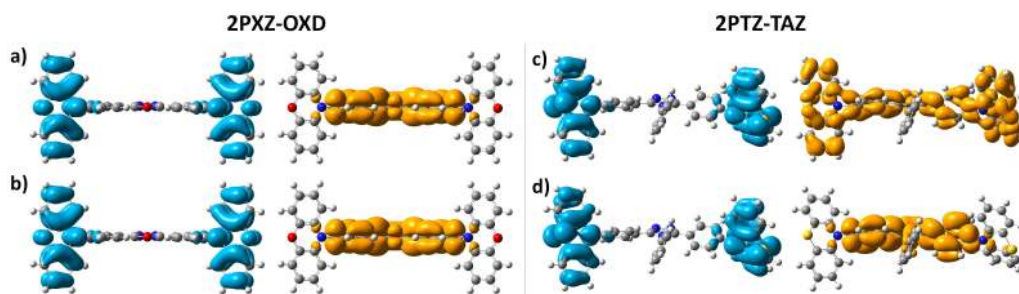
Figure 5: Hole (blue isocontour) and electron (orange isocontour) densities (cutoff=0.02 a.u.) obtained in the attachment/detachment formalism from TDA-PBE0-D3(BJ)/6-31G(d,p) calculations with the PCM module for solvent (toluene) for *(Left panel)* 2PXZ-OXD and *(Right panel)* 2PTZ-TAZ compounds associated with **a)** and **c)** T_1, and, **b)** and **d)** S_1 excited states.
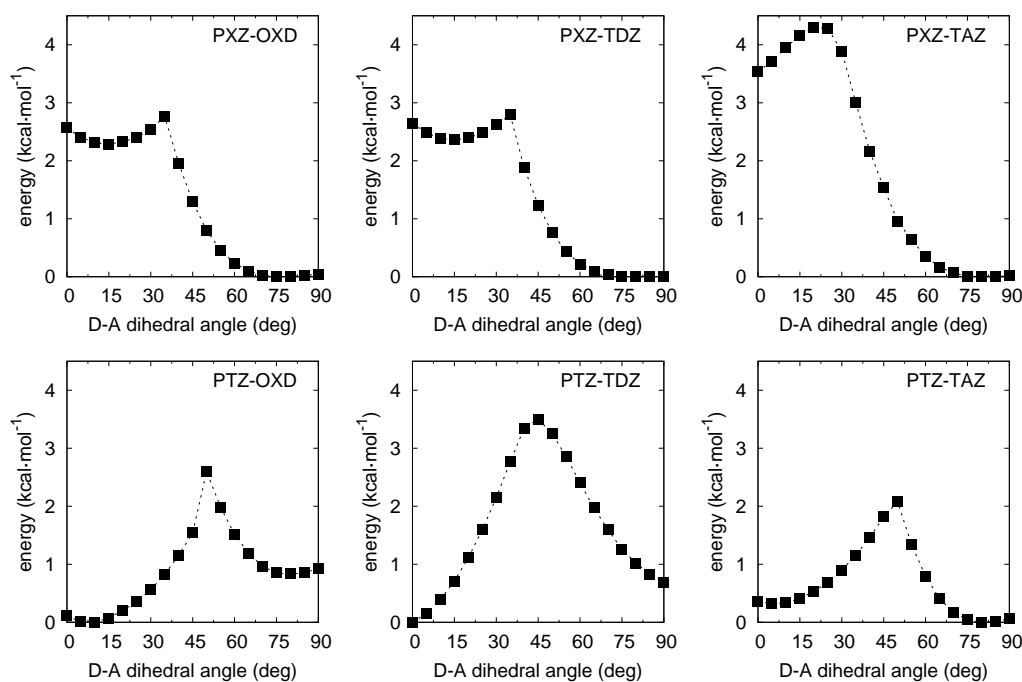

Figure 6: Torsion profiles calculated at the PBE0-D3(BJ)/6-31G(d,p) level of theory with the PCM module for solvent (toluene) between the different donors (PXZ and PTZ) and acceptors (OXD, TDZ, TAZ).
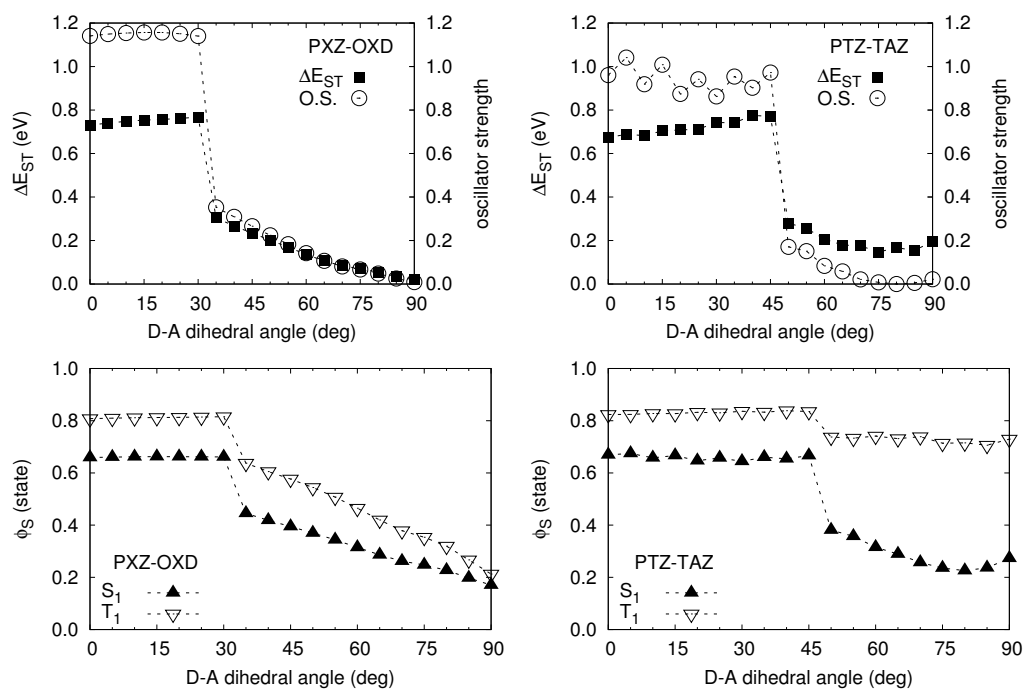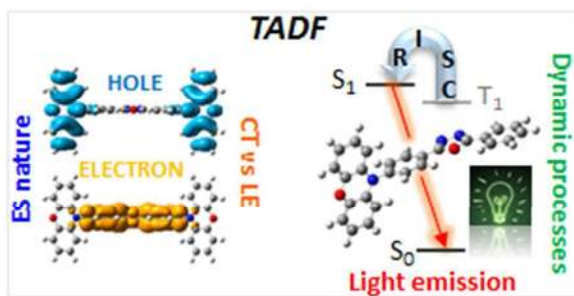
Figure 7: ΔE^{ST} and oscillator strength (O.S.) (*top panels*) and $\phi_S(S_1)$ and $\phi_S(T_1)$ (*bottom panels*) obtained at the TDA-PBE0-D3(BJ)/6-31G(d,p) level of theory with the PCM module for solvent (toluene), calculated for PXZ-OXD (*left panels*) and PTZ-TAZ (*right panels*) as a function of the torsion angle between their respective donor and OXD acceptor units.

41

In a theoretical study, we characterized the nature of the key excited states involved in TADF process of donor-acceptor compounds and show that light emission is enhanced by dynamic fluctuations of the donor-acceptor torsion resulting from flat torsional potentials.